https://doi.org/10.5194/egusphere-2026-1903
Preprint. Discussion started: 1 June 2026

Evaluation of angular resolution of the finite volume method on the predicted accuracy of wildfire thermal radiation

Yujia Sun, Shuai Pan
School of Atmospheric Physics, Nanjing University of Information Science & Technology, 210044, Nanjing, China
Correspondence to: Yujia Sun (yujia.sun@nuist.edu.cn)

Abstract. Thermal radiation is the dominant heat transfer mechanism in wildfires, governing both flame dynamics and fire spread through radiative preheating of unburned fuels. In physics-based wildfire models, the Finite Volume Method (FVM) is widely used to solve the 3D Radiative Transfer Equation. However, a fundamental contradiction exists between the demand for high-fidelity incident radiation predictions and the associated computational overhead. While previous research has predominantly focused on buoyancy-driven flames, this study systematically evaluates the impact of FVM angular resolution on the accuracy of surface incident radiation for both buoyancy-driven and wind-driven fire scenarios. Results show that low-resolution schemes (e.g., 16 azimuthal and 2 zenith angles) suffer from severe "ray effects"—non-physical numerical oscillations—leading to significant local heat flux errors. In calm atmosphere cases, a high resolution of at least 64-12 angles is required to eliminate artifacts and resolve the incident radiation correctly. In wind-driven scenarios where the flame is attached to the surface, the high-intensity radiation zone near the fire source is more tolerant of lower resolutions (e.g., 32-4), though far-field predictions remain sensitive. This research provides critical selection guidelines for angular discretization in wildfire radiation models.

1 Introduction

Wildfires have emerged as an increasingly severe global hazard (Senande-Rivera et al., 2022), and using physics-based combustion solvers for high-fidelity numerical modelling of fire dynamics and fire–atmosphere coupling processes is critically important and highly desirable (Wang et al., 2023). Thermal radiation plays an important role during the fire spread process (Dupuy and Maréchal, 2011). It affects the flame dynamics through radiative heating for fire temperature evolution and fire incident radiation on the adjacent surfaces (Liu et al., 2014). It is the dominant heat transfer mechanism for wildfire spread in calm and low velocity windy atmosphere (Liu et al., 2021).

Radiation modelling is a challenging task for fire combustion simulation (Liu et al., 2023). In atmospheric radiation, one-dimensional model is usually sufficient for calculation of radiative heat source or heat flux (Pincus et al., 2019). However, due to transient three-dimensional structure of the fire flame, three-dimensional radiative transfer equation (RTE) needs to be solved for fire radiation modelling. However, three-dimensional radiation modelling is computationally intensive in general

https://doi.org/10.5194/egusphere-2026-1903
Preprint. Discussion started: 1 June 2026

computational fluid dynamic codes because it needs to be solved by linear algebra solvers over many directions and spectral intervals (Sikic et al., 2019). For the spectral space of the thermal radiation transfer, there exists many global non-grey models for gas radiation (Nmira et al., 2020). For the angular space of the RTE, four methods are commonly used in fire modelling, the discrete ordinates method (DOM), the finite volume method (FVM), the sphere harmonic method, and the Monte Carlo method (Sun et al., 2022a). The DOM and FVM are the most popular ones due to its compromise between accuracy and efficiency, which depends highly on the amount of mesh these methods discretize the angular space into (Howell et al., 2010). It is commonly recognized that their accuracies increase with the angular resolution, at the cost of increasing computational time. Current literature shows that researchers frequently utilize low angular resolutions, such as the 48 to 80 solid angles employed by (Ahmed and Trouvé, 2021; Chatterjee et al., 2015; Chen et al., 2014; Maragkos et al., 2017), which are generally deemed sufficient for resolving radiative source terms and exchange within the flame core where radiation is nearly isotropic. However, as the focus extends to incident radiation on surrounding walls or distant surfaces, these low-resolution schemes often suffer from severe "ray effects"—non-physical numerical oscillations that can lead to local heat flux errors exceeding 100%. Consequently, studies by (Ma et al., 2020; Nmira et al., 2020; Sun et al., 2022b) have demonstrated that high-fidelity predictions of far-field wall heat flux require significantly finer discretization, such as the scheme or meshes exceeding 2000 rays, to resolve the vertical distribution of radiative flux correctly. This necessity highlights a fundamental contradiction between the demand for high-resolution accuracy and the associated computational cost, as CPU time for radiation solvers scales almost linearly with the number of control angles, making high-resolution coupled energy-radiation iterations prohibitively expensive.

Previous research has predominantly focused on the effect of angular resolution for buoyancy-driven flames (Sun et al., 2022; Maragkos et al., 2019), but there is few study for wind-driven flames, which is more relevant for wildfire conditions. It remains unclear how predicted accuracy of the incident radiation vary with angular resolution. Investigating how angular resolution impacts surface-incident radiation under varying flow configurations can provide useful selection guidelines or criterion for wildfire radiation simulation models. This study will focus on the FVM for solving the radiative transfer equation considering it is the most common models available in many CFD models, such as OpenFOAM (Open Field Operation And Manipulation) (The OpenFOAM Foundation, 2025), FDS (Fire Dynamic Simulator) (McGrattan et al., 2013) and ANSYS Fluent (ANSYS, 2020). It is to be noted that in some references the FVM in these solvers is called DOM since they both discretize the angular space into finite numbers, but we will use the FVM term in this work since they have quite differences in the angular discretization and in the conservation of radiation energy(Modest, 2013).

The purpose of this study is to clarify how the angular resolution of the finite volume method affects the prediction of surface incident radiation in wildfire radiation modelling. In particular, we aim to quantify the ray effects and local heat-flux errors caused by insufficient angular discretization, and to examine whether the required angular resolution differs between buoyancy-driven and wind-driven fire configurations. Formulations of the RTE and the FVM, and the detailed configuration

https://doi.org/10.5194/egusphere-2026-1903
Preprint. Discussion started: 1 June 2026

of two cases are described in section 2, and results of the incident radiation under different angular resolutions are presented and analysed in section 3, followed by main conclusions.

2 Equations and models

2.1 Radiative transfer equation

The radiative transfer equation (RTE) for the absorbing and emission medium is:

$$\frac{\mathrm{d}I_\eta(\hat{\mathbf{s}})}{\mathrm{d}s} = -\kappa_\eta I_\eta(\hat{\mathbf{s}}) + \kappa_\eta I_{\mathrm{b}\eta} \quad (1)$$

where κ_η is the spectral absorption coefficient, I_η is the spectral radiance, and $I_{\mathrm{b}\eta}$ is the blackbody intensity at wavelength η, $\hat{\mathbf{s}}$ is the ray direction.

The boundary condition for the radiative intensity is:

$$I_{\eta,\mathrm{w}}(\hat{\mathbf{s}}) = \varepsilon_{\mathrm{w}} I_{\mathrm{b}\eta,\mathrm{w}} + \frac{1-\varepsilon_{\mathrm{w}}}{\pi} \int_{\hat{n}\cdot\hat{\mathbf{s}}'<0} I_{\eta,\mathrm{w}}(\hat{\mathbf{s}}') \left|\hat{n}\cdot\hat{\mathbf{s}}'\right| \mathrm{d}\Omega' \quad (2)$$

For the high temperature fire flames, radiation heat transfer is dominated by the high temperature combustion products (mainly CO_2, H_2O and soot), whose radiative properties should be obtained from the HITEMP database, which is different from the requirement for common atmospheric radiation (Hogan and Bozzo, 2018).

For the non-grey modelling of high temperature gas radiation, the line-by-line model is computational expensive and not practical for the fire radiation. Instead, we adopted the efficient weighted-sum-of-grey-gases (WSGG) model in this work, which is widely used in combustion simulations. There exists many WSGG models for the radiation modelling of mixtures of CO_2 and H_2O, we used the model developed by Johansson et al. (Johansson et al., 2011), which is valid for a wide range of ratios of CO_2 and H_2O.

For the WSGG model, the RTE becomes:

$$\frac{\mathrm{d}I_j(\hat{\mathbf{s}})}{\mathrm{d}s} = -\kappa_j I_j(\hat{\mathbf{s}}) + a_j \kappa_j I_{\mathrm{bj}} \quad (3)$$

where index j denotes the j-th grey gas, and a_j is the weighting coefficient of the blackbody emission.

The incident radiation on a surface is calculated as:

$$Q_{in} = \sum_j \int_{\hat{n}\cdot\hat{\mathbf{s}}'<0} I_{\mathrm{j,w}}(\hat{\mathbf{s}}') \left|\hat{n}\cdot\hat{\mathbf{s}}'\right| \mathrm{d}\Omega' \quad (4)$$

which is summation of radiative intensity over all directions irradiate on a surface and all the grey gases.

https://doi.org/10.5194/egusphere-2026-1903
Preprint. Discussion started: 1 June 2026

90

2.2 Finite volume method for the RTE

The WSGG RTE is solved used the finite volume method for both the spatial discretization and angular discretization. For the angular discretization, the unit direction sphere is discretized into N_ϕ solid angles in the azimuthal direction and N_θ solid angles in the zenith direction, as shown in Fig. 1.

95 Integrating Eq. (3) over the control volume V and solid angle Ω_i yield:

$$\int_{\Omega_i}\int_V \frac{\mathrm{d}I_j(\hat{\mathbf{s}})}{\mathrm{d}s}\mathrm{d}V\mathrm{d}\Omega = -\int_{\Omega_i}\int_V \kappa_j I_j(\hat{\mathbf{s}})\mathrm{d}V\mathrm{d}\Omega + \int_{\Omega_i}\int_V a_j\kappa_j I_{\mathrm{bj}}\mathrm{d}V\mathrm{d}\Omega \tag{5}$$

By using Gauss's theorem and assuming that radiative intensity is constant in the control volume and over the solid angle, above equation can be further written as:

$$\sum_f I_{j,f}(\hat{\mathbf{s}})\mathbf{S}_f\cdot\overline{\mathbf{s}}_i + \kappa_j I_j(\hat{\mathbf{s}})V\Omega_i = a_j\kappa_j I_{\mathrm{bj}}V\Omega_i \tag{6}$$

100 where $\overline{\mathbf{s}}_i = \int_{\Omega_i}\hat{\mathbf{s}}\,\mathrm{d}\Omega$ is the average ray direction within the solid angle, and its value varies in different solid angles, depending on the azimuthal and zenith angles. The ray direction $\hat{\mathbf{s}}$ points to the centre of the solid angle.

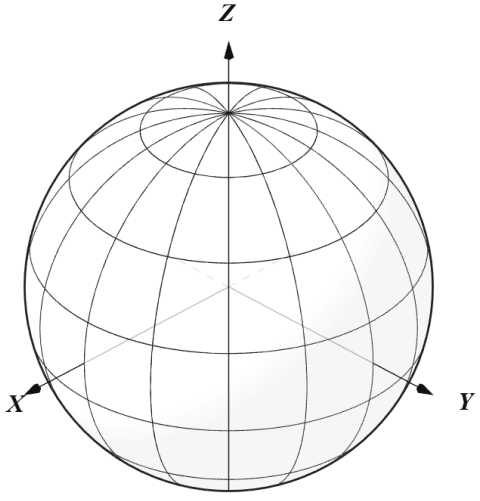

Figure 1 Schematic of the finite volume method for the angular discretization. The unit direction sphere is discretized into N_ϕ solid angles in the azimuthal direction and N_θ solid angles in the zenith direction.

105

The chose of numbers of N_ϕ and N_θ depends on the required accuracies of radiation quantities, such as radiative intensity at arbitrary direction, radiative heat source in the volume and incident radiation on a surface. We focus on the incident radiation

https://doi.org/10.5194/egusphere-2026-1903
Preprint. Discussion started: 1 June 2026

in this work because this term is important for radiative heating to unburn vegetables during fire spread. These two numbers will be varied to consider discrepancies of coarse angular resolution and fine angular resolution.

2.3 Studied cases

Two cases are considered in this work. The first case is a small-scale fire under calm atmosphere, and the second case is a moderate scale fire under windy atmosphere. The mesh grids with overlaid fire volume rendering for two cases are shown in figure 2. For the calm fire case, the diameter of the fuel inlet is 0.3 m, and the computational domain is a cylinder with diameter of 3 m and height of 3 m. This fire is buoyance driven and dominated by updraft flow. The mesh number for this case is 3.28 million. For the windy case, the fuel surface is 10 m in spanwise direction and 2 m in streamwise direction, and it is located 40 m from the computational inlet. The computational domain is 140 m length, 100 m wide, and 100 m high. Mesh is refined near the flame to capture strong gradients of temperature and velocities in this region, and total number of mesh is 4.02 million.

Both two fires are modelled by the fireFOAM model(Wang et al., 2011), which is designed specifically for fire modelling based on the framework of OpenFOAM and is publicly available. The fireFOAM model consists of fluid flow, combustion, heat transfer, species transport, turbulent and radiation sub-models. Note that spatial discretization method for all governing equations in fireFOAM are also called FVM. While for the radiation modelling, the FVM term usually denotes the angular discretization. Two angular discretization methods are available in fireFOAM for solving the radiation heat transfer, namely, the first order spheric harmonic method (P1), and the FVM. We focus on the FVM in this study because P1 is not accurate for fire radiation modelling(Sun and Zhang, 2018). Radiation heat transfer depends on temperature and concentrations of participating species. After finishing the fire simulations, temperatures, carbon dioxide mass fractions, and water vapor mass fractions are extracted from the results and used as inputs for the radiation modelling. As we focus on the radiation only, we did not perform coupled fire and radiation modelling with all the angular resolution cases. Instead, we perform the fire modelling with a relatively low angular resolution. Computational configuration for the overall combustion modelling can be found in (Sun et al., 2024) and not shown here. This strategy does not affect our purpose here because the predicted incident radiation has no influence on the combustion modelling, but can save us much computational time. To isolate the effect of angular resolution on the radiative transfer calculation, a radiation-only solver, hereafter referred to as radFoam, was developed by modifying the fireFOAM solver. In radFoam, the governing equations for the reacting flow field, including continuity, momentum, pressure, enthalpy/energy, species/combustion, turbulence, and multiphase sub-models, were removed or disabled. The radiation-model infrastructure was retained, and only the FVM for the radiative transfer equation was solved on prescribed thermochemical fields. The solver can be found at (Sun, 2026). By doing so, we only needed to change N_ϕ and N_θ to get the incident radiation for all the angular resolutions.

https://doi.org/10.5194/egusphere-2026-1903
Preprint. Discussion started: 1 June 2026

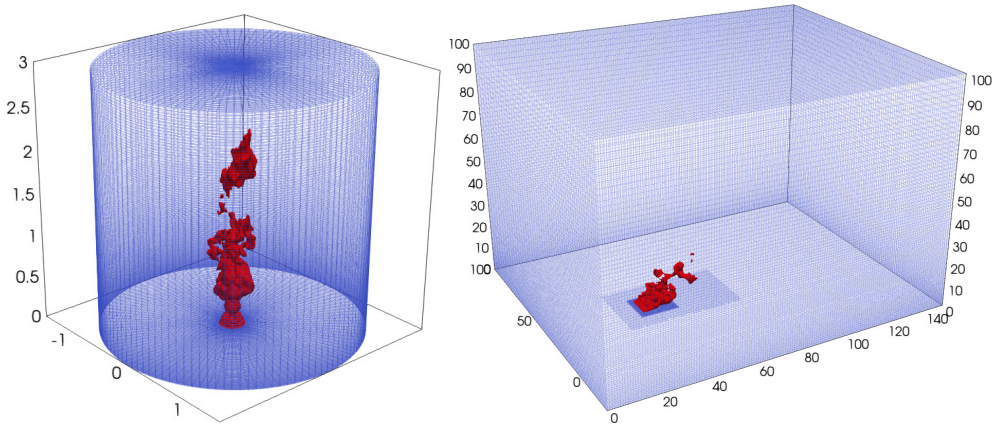

Figure 2: Schematic of the mesh grids for the calm and windy atmosphere cases. Unit of length is m.

3 Results

3.1 Calm atmosphere

The first case is a buoyant driven fire under calm atmosphere, and Fig. 3 presents a typical transient temperature contour and velocity vectors. The high temperature zone is highly non-uniform and oscillates due to Kelvin-Helmholtz instability. The maximum temperature at this specific time reaches 1738 K, which is just about the ground surface. This irregular distribution of temperature is directly related to the ray effect of the finite volume method of the radiation transfer. The maximum velocity is about 6.2 m s^{-1} and occurs at a relatively higher height compared to the temperature. Air entrainment effect can be observed near the edge of the fire plume. The velocity field is not a direct input to the RTE in the present decoupled radiation-only calculations. For a prescribed thermochemical field, the FVM-predicted incident radiation is controlled by the temperature, participating-species concentrations, radiative properties, boundary conditions, spatial grid, and angular discretization. Therefore, the velocity field shown in Fig. 3 does not directly affect the numerical performance of the FVM or the ray effects analysed here. Nevertheless, in fully coupled fire simulations, velocity can indirectly affect radiation by changing the flame shape, temperature field, and species distributions (Modest, 2013).

Figure 4 shows the transient volume rendering of the flame by temperature (>420 K). This temperature distribution shows the puffing characteristic of the buoyance-driven flame, which causes small-scale vortex near the ground surface, and larger scale vortex at higher locations. This separation of high temperature vortexes will also intensify the ray effect of the finite volume method, which will be discussed next. Due to the unit Lew number assumption, distributions of carbon dioxide and water vapor are same to that of the temperature, and are not shown here.

https://doi.org/10.5194/egusphere-2026-1903
Preprint. Discussion started: 1 June 2026

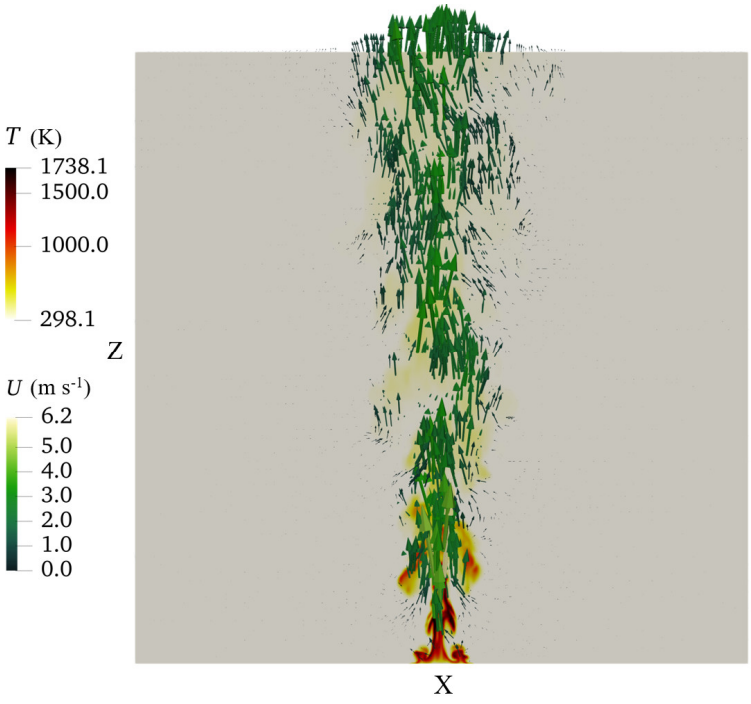

Figure 3: Transient temperature contour and velocity vectors for the calm atmosphere case.

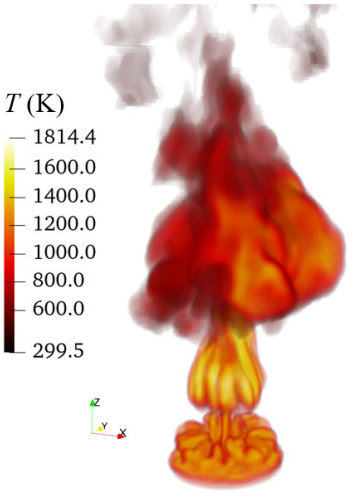

Figure 4: Transient volume rendering of the flame by temperature (>420 K) of the calm fire case.

https://doi.org/10.5194/egusphere-2026-1903
Preprint. Discussion started: 1 June 2026

Figure 5 shows the incident radiation on the ground surface corresponding to the temperature distributions in Fig. 3 and 4. The numbers in each sub-figure denote the mesh size in the azimuthal and zenith directions respectively. When the angular resolution is 16-2, we can clearly observe the "ray effect" due to inadequate angular discretization. There are exactly 16 false rays originating from the fuel centre, which is related to the mesh size in the azimuthal direction. This false ray effect becomes larger towards outer side, and is not obvious at the edge of the fuel region. Along the radial direction, there are generally three local maximums, the first one is located near the edge of the flame, the second one is located at the middle location, and the third one is located at out regions (white flag shape). These three levels of incident radiation correspond to the three levels of vortex structures in Fig. 4. However, this is also physically false and caused by the ray effect in the zenith direction, which has not 2 mesh. When the mesh size is doubled to 32-4, these ray effects are reduced but still observable. Another significant change is that incident radiation near the edge of the fuel become larger and wider. There is also a weak local maximum at the northeast direction of the fuel region, which is possibly because the flame is slightly inclined towards this direction. Keeping the zenith mesh size unchanged and increasing the azimuthal mesh size to 40, the ray effect in the azimuthal direction is further reduced, but still can be seen. When we further increase the azimuthal mesh size to 64, the azimuthal ray effect vanishes, but the zenith ray effect still exists. It becomes less obvious when the zenith mesh size is increased to 12. At the mesh size, the local maximum at the northeast direction of the fuel region vanishes, and the incident radiation become smooth in both azimuthal and radial direction.

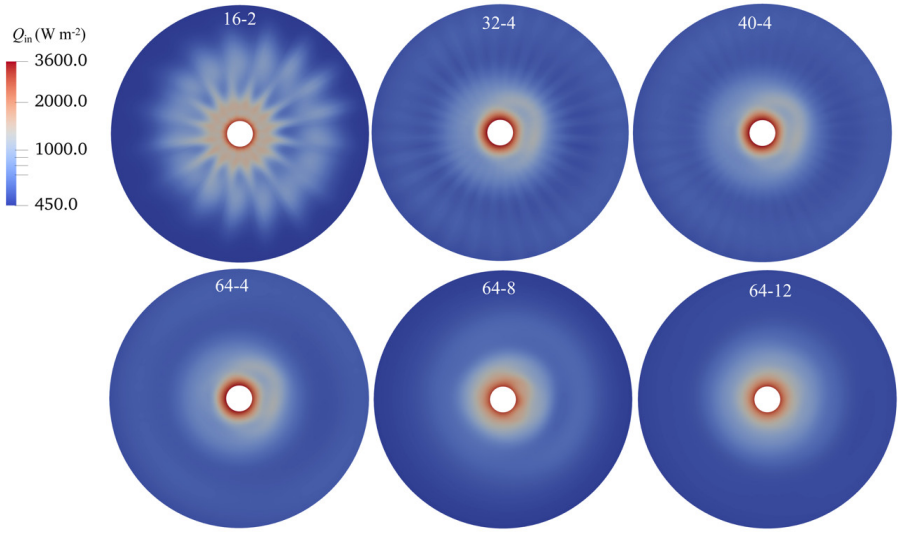

Figure 5: Transient incident radiation on the ground surface for the calm fire case. The numbers in each sub-figure denote the mesh sizes in the azimuthal and zenith directions.

To further reveal the effect of angular resolution, figure 6 presents the predicted incident radiation along y=0 m and y=0.3 m. The former line crosses the fuel centre, while the latter line is 0.3 m away from the centre. Form Fig. 6(a), angular resolution

https://doi.org/10.5194/egusphere-2026-1903
Preprint. Discussion started: 1 June 2026

has variable differences at different locations. At x<=0.15 m, the incident radiation is in the range of 2500-3000 W m^{-2}, and all the resolutions predicts close results. However, the incident radiation becomes oscillating and deviations between different angular meshes become larger at larger *x* locations. The incident radiation profile of 16-2 mesh has the largest amplitude, especially at *x*=0.9 m. Increasing the angular meshes will generally decrease this amplitude. However, increasing angular mesh in only one direction does not necessarily guarantee improved accuracies. For example, incident radiation profiles of 32-4, 40-4 and 64-4 are almost the same along the x direction. Increasing the angular mesh in the zenith direction tends to decrease the oscillating behaviour of radiation, which can be seen from the profiles of 64-4, 64-8 and 64-12. The incident radiation profile of 64-12 is the smoothest, indicating this number is sufficient for eliminate the ray effect. For the incident radiation profile along *y*=0.3 m, the oscillating is also generally reduced with increasing the angular resolution. All the resolution can predict the peak location well but has varied discrepancies. Compared to the predicted incident radiation of 64-12, those of 16-2,48-6, and 64-8 are over-predicted, while those of other are under-predicted.

To sum up, from results of figure 6, the azimuthal mesh size should be 64 or more reduce the ray effect, and the zenith mesh size should be 12 or more to obtain smooth incident radiation profiles. This would require substantial computational resources for solving the RTE, which will be discussed in the next section.

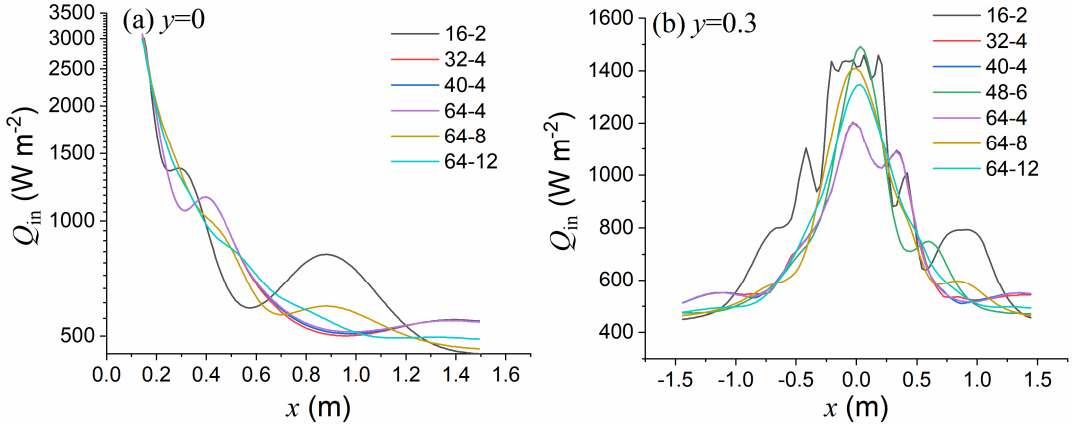

Figure 6: Effect of angular resolution on the incident radiation along (a) *y*=0 and (b) *y*=0.3 m for the calm fire case.

3.2 Windy atmosphere

The second case is a wind-driven fire under windy atmosphere, as shown in Fig. 7. This case has a large fuel region and the flame is blown toward downward by the wind. The updraft of the fire plume induces a maximum velocity of 12.7 m s^{-1}, and the plume is inclined downstream. At the windward side of the flame, vortex is formed due to Keven-Helmholtz instability. Downdraft is also obvious at the windward side. At the downstream of the flame, velocity become smaller due to flow stagnation of spanwise air entrainments at the middle plane. Although the velocity field does not directly affect the radiation heat transfer, it has indirect effect on the radiation process through its influence on the temperature field. The high temperature region is limited to a smaller region near the fuel surface compared to the velocity field, and is especially larger

https://doi.org/10.5194/egusphere-2026-1903
Preprint. Discussion started: 1 June 2026

at the leeside of the fuel surface, as shown in Fig. 8. The flame touches the surface and the flame drag length (the length of the flame attachment) is comparable to the fuel width. This flame feature has significant effect on the radiation heat transfer to the ground surface as the attached high temperature combustion products are very close to the surface compared to that of the calm atmosphere case, which can tremendously enhance the incident radiation. The high-temperature region extends from the fuel rear edge into the air downstream at a distance equivalent to several fuel widths, with decreasing temperature. This region will also induce high incident radiation to the ground surface.

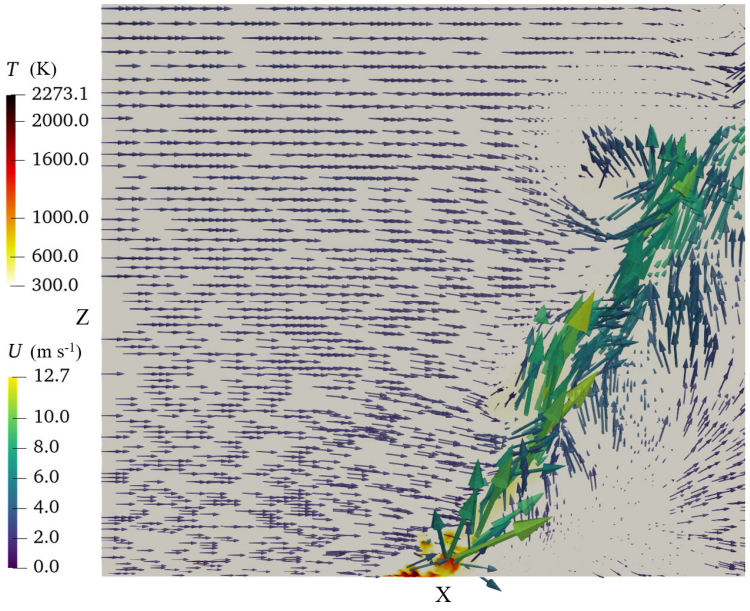

Figure 7: Transient temperature contour and velocity vectors for the windy atmosphere case.

https://doi.org/10.5194/egusphere-2026-1903
Preprint. Discussion started: 1 June 2026

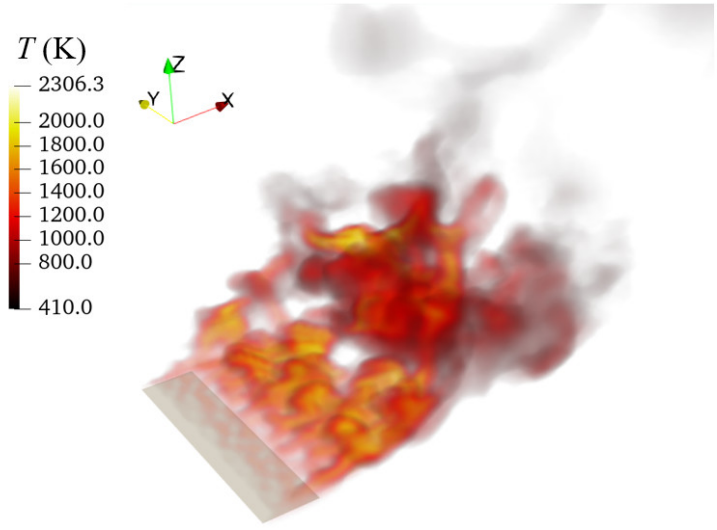

230 Figure 8: Transient volume rendering of the flame by temperature (>420 K) of the windy fire case.

Figure 9 shows the incident radiation on the ground surface corresponding to the temperature distributions in Fig. 7 and 8. The numbers in each sub-figure denote the mesh size in the azimuthal and zenith directions respectively. The maximum incident radiation reaches about 150000 W m^{-2} at downstream of the fuel rear edge. This value is significantly larger than
235 that of the calm fire case due to the close distance between the flame and the surface. All the resolution cases predict similar incident radiation distribution, whose value is largest at about one fuel width away from the fuel rear edge, and gradually decreases downstream. The incident radiation at the windward side of the fuel surface is much smaller. The non-uniform distribution of radiation (with local peaks and troughs) near the rear edge of the fuel surface is due to irregular flame shape above the ground, which results from the peak and trough structure of the wind and fire interaction. The result of 8-2 also
240 have clear local peaks and troughs at the range of 3000-10000 W m^{-2}. This is consequence of false ray effect of the finite volume method, and should not be interpreted as result of the peak and trough structure of the flame. This ray effect decreases as the resolution increases to 16-2. A local minimum can be observed at point (50 m, 45 m) for these two resolutions but vanishes for other resolutions, indicating that it is caused by the inadequate resolution in the zenith direction. The ray effect also vanishes starting from 32-4. Further increasing resolution has small effect on the radiation distribution
245 near the fuel surface. For the region away from the fuel surface, finer resolutions predict larger values, which implies that insufficient resolution tends to falsely accumulates radiation heat near the fire source. Taken results of 40-6 and 64-12 as an example, incident radiation at the windward side and flank sides of the fuel surface is smoother for the 64-12 case, indicating a more diffused radiation distribution. This variation of predicted radiation may affect the fire spread rate calculation for back fire and flank fires, and also affect radiation pre-heating at further downstream.
250

https://doi.org/10.5194/egusphere-2026-1903
Preprint. Discussion started: 1 June 2026

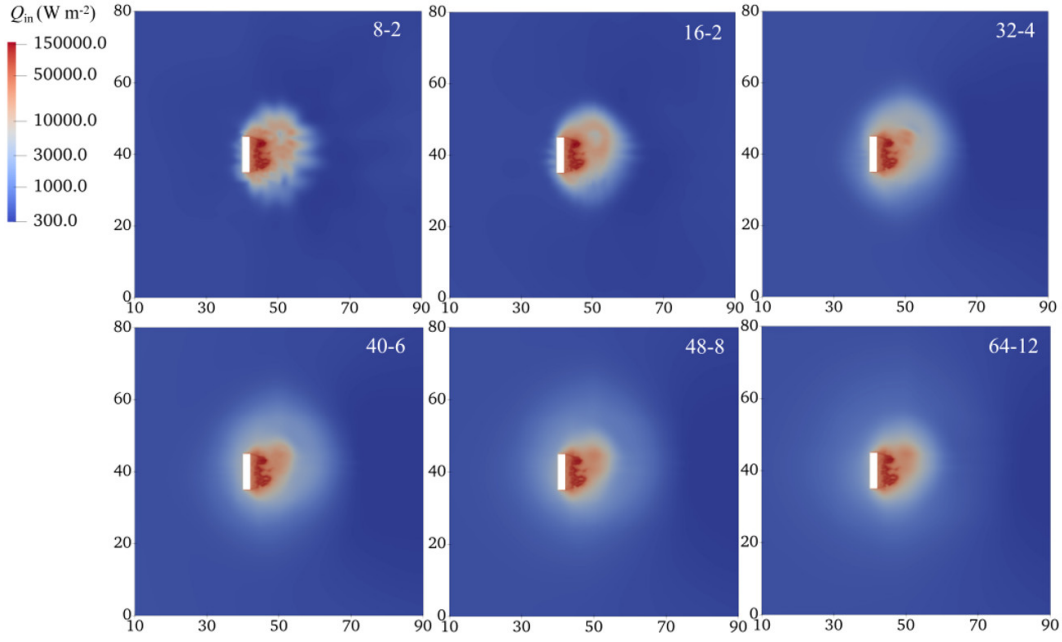

Figure 9: Transient incident radiation on the ground surface for the windy fire case. The numbers in each sub-figure denote the mesh sizes in the azimuthal and zenith directions.

Figure 10 presents the predicted incident radiation along x=54 m and x=45 m. The former line is further away from the fuel region, and hence has smaller incident radiation, as shown in Fig. 10(a). The radiation is largest at y=40 m, and decreases gradually toward flank sides. It is clear that coarse resolution over-predicts the radiation at the centre and under-predicts at flank sides. The ray effect is most obvious at the centre. With increasing the resolution, the ray effect is reduced and tends to move from the centre to sides. Increasing the resolution will generally smooth the incident profile. At x=45 m, the incident radiation can reach about 150000 W m^{-2}, and also shows a unimodal pattern. The incident radiation is smoother for finer resolution, but decreases sharply from the centre to the sides for all resolutions. Its value reduces from 150000 W m^{-2}, at the centre to about 500 W m^{-2} in less than 20 m. The incident radiations near the centre are oscillating for all resolutions are very close to each other, especially for resolutions larger than 32-4. This implies that for incident radiation prediction in this region, resolution of 32-4 is sufficient to get angular mesh independent results. However, it still has large errors at locations further away from the centre. For windy fire case, fire spread is usually dominant along the wind direction, which is coincide with the regions with large incident radiation as in Fig.10(b). This may lead to an assumption that we do not need very fine mesh (like 16-12) to predict the incident radiation accurately for a large domain. Middle resolution (like 32-4) may be enough to predict the radiation heat transfer for the fire spread calculation. But its effect on the fire spread needs further systematic investigations.

https://doi.org/10.5194/egusphere-2026-1903
Preprint. Discussion started: 1 June 2026

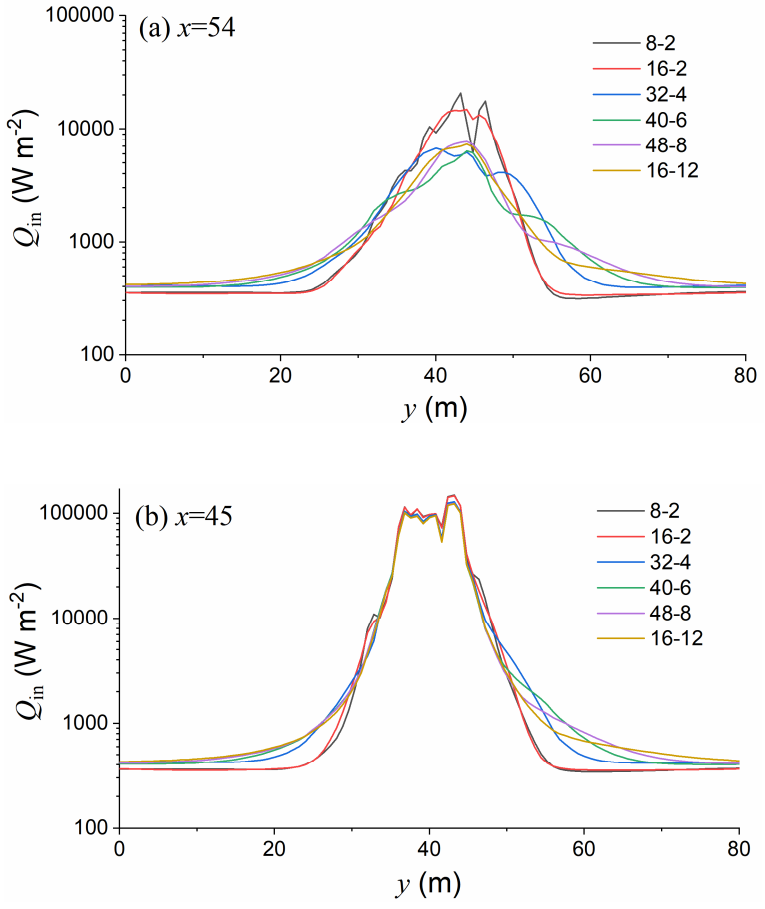

Figure 10 Effect of angular resolution on the incident radiation along (a) x=54 m and (b) x=45 m for the wind fire case.

To assess the effect of angular resolutions on the computational performance of the radiation modelling, table 1 and 2 present computational time and memory requirement for two cases, especially for the 64-12 case. It can be seen that the computational time increases with increasing the resolution, ranging from about 1 minute to 16 minutes. As the radiation modelling is only small part of the fire modelling, it is not effective to use fine resolution (such as 64-12). A common way to reduce computational time of radiation modelling is solving the RTE once for 100 or more energy iterations. Except from the computational time, finer resolution needs more memory. For example, the radiation simulation was successful for 64-8 resolution using 2 computational nodes, but failed for 64-12 resolution, and we had to use 3 computational nodes to successfully run the code. Each node of the cluster has memory of 500 G, indicating that 64-12 case needs more than 1 T memory to run. In fact, a total number of 3840 (64×12×5) variables are needed for the radiative intensities, which also need large storages for the results.

https://doi.org/10.5194/egusphere-2026-1903
Preprint. Discussion started: 1 June 2026

Table 1: Computational time and memory requirements for the calm fire case

Resolution	**Time/ s**	**Memory**
40-4	56	2 node /128CPU
64-4	98	2 node /128CPU
64-8	284	2 node /128CPU
64-12	**984**	**3 node /192CPU**

Table 2: Computational time and memory requirements for the windy fire case

Resolution	**Time/ s**	**Memory**
32-4	111	1node/64CPU
40-6	786	1 node /64CPU
48-8	285	1 node /64CPU
64-12	**590**	**4 node /256CPU**

4 Conclusions

Three-dimensional radiation modelling is an important component of wildfire simulation. The finite volume method is the most common method to solve the 3D RTE, but its performance depends highly on the angular resolution. To evaluate how the predicted accuracy of the FVM vary with the angular resolution, this work assesses the incident radiation on the ground surface for two fire cases, a buoyancy-driven fire and a wind-driven fire. Based on the Large Eddy Simulation (LES) and multi-resolution radiation analysis, following conclusions are drawn:

(1) The impact of angular resolution is dependent on the flame shape. In buoyancy-driven (calm) fires, the incident radiation is extremely sensitive to both azimuthal and zenith discretization due to the oscillating vortex structures. A resolution of 64-12 is necessary to obtain smooth and physically realistic incident profiles. In contrast, for wind-driven fires, the flame

https://doi.org/10.5194/egusphere-2026-1903
Preprint. Discussion started: 1 June 2026

attachment to the ground surface creates a high-flux zone that reaches independent results at a moderate resolution of 32-4, although ray effects persist in the low-intensity far-field regions.

(2) There is a linear increase in computational time and memory consumption with higher angular resolutions. High-resolution cases (e.g., 64-12) can require much more memory and significantly increase total simulation time, which is often prohibitively expensive for large-scale wildfire coupling models.

In practical wildfire simulations, the FVM angular resolution should not be chosen as a fixed universal value, but should depend on the flame configuration and the target application. For buoyancy-driven fires, the present results indicate that a resolution of at least 64-12 is needed to suppress ray effects and obtain smooth ground incident-radiation profiles. For wind-driven fires with flame attachment to the surface, the high-intensity near-source radiation region is less sensitive to angular resolution, and a moderate resolution of 32-4 can provide a practical compromise for predicting forward fire-spread-related radiative heating. However, for far-field radiation, flank or backing fire preheating, and thermal exposure assessment, higher angular resolutions such as 40-6, 48-8, or 64-12 are recommended. Very low resolutions, such as 16-2, should be avoided except for preliminary tests, because they may generate non-physical ray effects and misleading local heat-flux distributions. Considering the substantial increase in computational time and memory demand at high angular resolutions, the 64-12 configuration is more appropriate for benchmark, sensitivity, or decoupled post-processing calculations, whereas 32-4 may be more suitable for routine large-scale coupled wildfire simulations.

Despite providing critical guidelines for angular discretization in wildfire modelling, this study has certain limitations that should be addressed in future research. First, this study utilized a decoupled "post-processing" approach to evaluate incident radiation; while efficient, it may overlook the complex transient feedback between radiative preheating and flame dynamics that occurs during real fire spread. Second, the focus was limited to non-sooting flames, whereas real-world wildfires involve heavy soot production and smoke plumes, which significantly alter the optical thickness and may impose different angular resolution requirements to resolve high-intensity radiation through participating media.

Future work should explore the development of adaptive angular refinement algorithms that dynamically increase resolution only in regions sensitive to ray effects, such as the far-field or near-surface attachment zones. Additionally, it is essential to systematically investigate how these angular discretization choices directly influence the predicted fire spread rate, integrating more complex pyrolysis models and soot-radiation physics to further its effect on the wildfire predictive capabilities.

https://doi.org/10.5194/egusphere-2026-1903
Preprint. Discussion started: 1 June 2026

Code, data, or code and data availability

The OpenFOAM (version 1912) software, radFoam solver, incident radiation dataset for the two cases and OpenFOAM configurations are available at Zenodo: https://doi.org/10.5281/zenodo.19389082 (Sun, 2026) .

Author contributions

YJS developed the model code, YJS performed the simulations, YJS and SP analysed the results and prepared the figures, YJS prepared the manuscript with contributions from all co-authors.

Competing interests

There are no potential conflicts of interest.

Acknowledgements

The simulation is performed on the High-Performance Computing Center of Nanjing University of Information Science & Technology.

Financial support

This study is founded by the National Natural Science Foundation of China (No. 42405078) and the Natural Science Foundation of Jiangsu Province (BK20220461).

References

Ahmed, M. M. and Trouvé, A.: Large eddy simulation of the unstable flame structure and gas-to-liquid thermal feedback in a medium-scale methanol pool fire, Combust. Flame, 225, 237–254, https://doi.org/10.1016/j.combustflame.2020.10.055, 2021.

ANSYS: ANSYS Fluent Theory Guide, Canonsburg, PA, 2020.

Chatterjee, P., Wang, Y., Meredith, K. V., and Dorofeev, S. B.: Application of a subgrid soot-radiation model in the numerical simulation of a heptane pool fire, Proc. Combust. Inst., 35, 2573–2580, https://doi.org/10.1016/j.proci.2014.05.045, 2015.

https://doi.org/10.5194/egusphere-2026-1903
Preprint. Discussion started: 1 June 2026

Chen, Z., Wen, J., Xu, B., and Dembele, S.: Large eddy simulation of a medium-scale methanol pool fire using the extended eddy dissipation concept, Int. J. Heat Mass Transf., 70, 389–408, https://doi.org/10.1016/j.ijheatmasstransfer.2013.11.010, 2014.

Dupuy, J. L. and Maréchal, J.: Slope effect on laboratory fire spread : contribution of radiation and convection to fuel bed preheating, Int. J. Wildl. Fire, 20, 289–307, 2011.

Hogan, R. J. and Bozzo, A.: A Flexible and Efficient Radiation Scheme for the ECMWF Model, J. Adv. Model. Earth Syst., 10, 1990–2008, https://doi.org/https://doi.org/10.1029/2018MS001364, 2018.

Howell, J. R., Menguc, M. P., and Siegel, R.: Thermal Radiation Heat Transfer, 5th ed., CRC press, Boca Raton, 2010.

Johansson, R., Leckner, B., Andersson, K., and Johnsson, F.: Account for variations in the H2O to CO2 molar ratio when modelling gaseous radiative heat transfer with the weighted-sum-of-grey-gases model, Combust. Flame, 158, 893–901, https://doi.org/10.1016/j.combustflame.2011.02.001, 2011.

Liu, F., Consalvi, J. L., and Nmira, F.: The importance of accurately modelling soot and radiation coupling in laminar and laboratory-scale turbulent diffusion flames, Combution and Flame, 112573, https://doi.org/10.1016/j.combustflame.2022.112573, 2023.

Liu, N., Wu, J., Chen, H., Xie, X., Zhang, L., Yao, B., Zhu, J., and Shan, Y.: Effect of slope on spread of a linear flame front over a pine needle fuel bed : experiments and modelling, Int. J. Wildl. Fire, 23, 1087–1096, 2014.

Liu, N., Lei, J., Gao, W., Chen, H., and Xie, X.: Combustion dynamics of large-scale wildfires, Proc. Combust. Inst., 38, 157–198, https://doi.org/10.1016/j.proci.2020.11.006, 2021.

Ma, L., Nmira, F., and Consalvi, J. L.: Large Eddy Simulation of medium-scale methanol pool fires - effects of pool boundary conditions, Combust. Flame, 222, 336–354, https://doi.org/10.1016/j.combustflame.2020.09.007, 2020.

Maragkos, G., Beji, T., and Merci, B.: Advances in modelling in CFD simulations of turbulent gaseous pool fires, Combust. Flame, 181, 22–38, https://doi.org/10.1016/j.combustflame.2017.03.012, 2017.

McGrattan, K., McDermott, R., Weinschenk, C., and Forney, G.: Fire Dynamics Simulator, Technical Reference Guide, Sixth Edition, Special Publication (NIST SP), Gaithersburg, MD, https://doi.org/https://doi.org/10.6028/NIST.sp.1018, 2013.

Modest, M. F.: Radiative Heat Transfer, 3rd ed., Academic Press, New York, 2013.

Nmira, F., Ma, L., and Consalvi, J. L.: Influence of gas radiative property models on Large Eddy Simulation of 1 m methanol pool fires, Combust. Flame, 221, 352–363, https://doi.org/10.1016/j.combustflame.2020.08.005, 2020.

Pincus, R., Mlawer, E. J., and Delamere, J. S.: Balancing Accuracy, Efficiency, and Flexibility in Radiation Calculations for Dynamical Models, J. Adv. Model. Earth Syst., 11, 3074–3089, https://doi.org/https://doi.org/10.1029/2019MS001621, 2019.

Senande-Rivera, M., Insua-Costa, D., and Miguez-Macho, G.: Spatial and temporal expansion of global wildland fire activity in response to climate change, Nat. Commun., 13, 1208, https://doi.org/10.1038/s41467-022-28835-2, 2022.

Sikic, I., Dembele, S., and Wen, J.: Non-grey radiative heat transfer modelling in LES-CFD simulated methanol pool fires, J. Quant. Spectrosc. Radiat. Transf., 234, 78–89, https://doi.org/10.1016/j.jqsrt.2019.06.004, 2019.

https://doi.org/10.5194/egusphere-2026-1903
Preprint. Discussion started: 1 June 2026

Sun, Y.: Dataset for the "Evaluation of angular resolution of the finite volume method on the predicted accuracy of wildfire thermal radiation," https://doi.org/10.5281/zenodo.19389082, 2026.

Sun, Y. and Zhang, X.: Contributions of gray gases in SLW for non-gray radiation heat transfer and corresponding accuracies of FVM and P1 method, Int. J. Heat Mass Transf., 121, 819–831, https://doi.org/10.1016/j.ijheatmasstransfer.2018.01.045, 2018.

Sun, Y., Shen, H., Zheng, S., and Jiang, L.: A hybrid non-gray gas radiation heat transfer solver based on OpenFOAM, J. Quant. Spectrosc. Radiat. Transf., 281, 108105, https://doi.org/10.1016/j.jqsrt.2022.108105, 2022a.

Sun, Y., Yu, Y., Jiang, L., and Zheng, S.: Transient three-dimensional radiative heat transfer analysis of a turbulent diffusion flame-with a focus on the effect of angular discretization scheme, Int. Commun. Heat Mass Transf., 137, 106300, https://doi.org/10.1016/j.icheatmasstransfer.2022.106300, 2022b.

Sun, Y., Zheng, S., and Liu, C.: Interaction of the flow and flame dynamics of a line wildfire in the atmospheric wake flow of a ridge, Phys. Fluids, 36, https://doi.org/10.1063/5.0203409, 2024.

The OpenFOAM Foundation: OpenFOAM, https://openfoam.org/, 2025.

Wang, Q., Ihme, M., Linn, R. R., Chen, Y. F., Yang, V., Sha, F., Clements, C., McDanold, J. S., and Anderson, J.: A high-resolution large-eddy simulation framework for wildland fire predictions using TensorFlow, Int. J. Wildl. Fire, 32, 1711–1725, https://doi.org/10.1071/WF22225, 2023.

Wang, Y., Chatterjee, P., and de Ris, J. L.: Large eddy simulation of fire plumes, Proc. Combust. Inst., 33, 2473–2480, 2011.